Molecular Crystals and Liquid Crystals
Publication details, including instructions for authors and subscription information:
http://www.tandfonline.com/loi/gmcl20

Hydrothermal Synthesis, Crystal Structure of Five Novel Complexes Based on 4-Chlorophenyloxyacetic Acid

Long Li [a] , Kaisheng Diao [a b] , Yuqiu Ding [a] & Xianhong Yin [a]
[a] College of Chemistry and Chemical Engineering , Guangxi University for Nationalities , Nanning , People's Republic of China
[b] Guangxi Key Laboratory of Chemistry and Engineering of Forest Products , Guangxi University for Nationalities , Nanning , People's Republic of China
Published online: 22 Apr 2013.

To cite this article: Long Li , Kaisheng Diao , Yuqiu Ding & Xianhong Yin (2013) Hydrothermal Synthesis, Crystal Structure of Five Novel Complexes Based on 4-Chlorophenyloxyacetic Acid, Molecular Crystals and Liquid Crystals, 575:1, 173-187, DOI: 10.1080/03610918.2013.767739

To link to this article: http://dx.doi.org/10.1080/03610918.2013.767739

Mol. Cryst. Liq. Cryst., Vol. 575: pp. 173–187, 2013

ISSN: 1542-1406 print/1563-5287 online
DOI: 10.1080/03610918.2013.767739

Hydrothermal Synthesis, Crystal Structure of Five Novel Complexes Based on 4-Chlorophenyloxyacetic Acid

LONG LI,[1] KAISHENG DIAO,[1,2] YUQIU DING,[1] AND XIANHONG YIN[1,*]

[1]College of Chemistry and Chemical Engineering, Guangxi University for Nationalities, Nanning, People's Republic of China
[2]Guangxi Key Laboratory of Chemistry and Engineering of Forest Products, Guangxi University for Nationalities, Nanning, People's Republic of China

*Five new metal–organic complexes of the formula $[Pb_3L_5(2,2'\text{-bipy})_2(NO_3)(H_2O)]_n$ **1**, $[Cd_2L_4(1,10\text{-Phenanthroline})_2]$ **2**, $[Mn_2L_4(1,10\text{-Phenanthroline})_2]$ **3**, $[Mn_3L_6(2,2'\text{-bipy})_2]$ **4**, and $[PbL_2(H_2O)]_n$ **5** [HL = 4-chlorophenyloxyacetic acid] have been synthesized and characterized by IR method, elemental analysis, X-ray powder diffraction (XRPD) analysis, fluorescence spectroscopy method, and single-crystal X-ray diffraction techniques. X-ray structure analysis reveals that complex **1** is 1D chain polymer, complex **5** is 2D network polymer, while complex **2**, **3**, and **4** are all 0D structure. The L ligand have many kinds of coordination mode, which make these complexes have different configuration. The weak C–H···O and π–π interactions are also very important, the mononuclear or multinuclear crystal units of these complexes can be packed through them. Moreover, all these complexes exhibit fluorescence.*

Keywords 4-chlorophenyloxyacetic acid; fluorescence; hydrothermal synthesis

Introduction

As far as we know, halogen phenoxyl carboxylates were widely used as excellent pesticide and the plant auxin in agriculture in recent decades [1–4]. However, it can also pollutes our environment and results in the intoxication of animals and humans [5]. In order to decrease these intoxications, many researches focused on the degradation of the pesticide. Coordinating halogen phenoxyl carboxylates with metal ion is a good way. Besides, the self-assembly of metal ions and halogen phenoxyl carboxylates ligands have made progress by detailed studies of their structural characteristics, such as diverse coordination modes and conformations, and their potential applications as catalysts, luminescent, sorption, magnetic materials, and biological reagents [6–10]. As bridging ligands, halogen phenoxyl carboxylates, are of huge interest in the construction of polymeric coordination architectures not only because the fact that these polymers have a wide range of structural diversities and potential applications as porous materials and magnetic materials, but also

*Address correspondence to Xianhong Yin, College of Chemistry and Chemical Engineering, Guangxi University for Nationalities, Nanning 530006, People's Republic of China. E-mail: llgxmd@163.com

because these ligands exhibit rich coordination chemistry. 4-chlorophenyloxyacetic acid is a typical halogen phenoxyl carboxylate ligand, to our knowledge, many of the most interesting metal–organic polymers with one-, two-, and three-dimensional networks have been engineered using anionic, carboxylate ligands, L has one flexible acetate.

However, no literatures related to the titled complexes have been published. Herein, we report the synthesis, structure of five new complexes, $[Pb_3L_5(2,2'\text{-bipy})_2(NO_3)(H_2O)]_n$ **1**, $[Cd_2L_4(1,10\text{-Phenanthroline})_2]$ **2**, $[Mn_2L_4(1,10\text{-Phenanthroline})_2]$ **3**, $[Mn_3L_6(2,2'\text{-bipy})_2]$ **4**, and $[PbL_2(H_2O)]_n$ **5** [HL = 4-chlorophenyloxyacetic acid]. In addition, we investigate the fluorescence of these complexes.

Experimental

Materials and Instrumentation

All reagents and solvents were used directly as supplied commercially without further purification. Elemental analysis for C, H, and N was carried out on a Perkin–Elmer 2400 II elemental analyzer. The FT-IR spectrum was obtained on a PE spectrum one FT-IR spectrometer Fourier transform infrared spectroscopy in the 4000–400 cm^{-1} regions, using KBr pellets. The X-ray powder diffraction (XRPD) was recorded on a XD-3 diffractometer (Beijing, China) at 36 kV, 25 mA for a Cu-target tube, and a graphite monochromator. Simulation of the XRPD spectra was carried out by the single-crystal data and

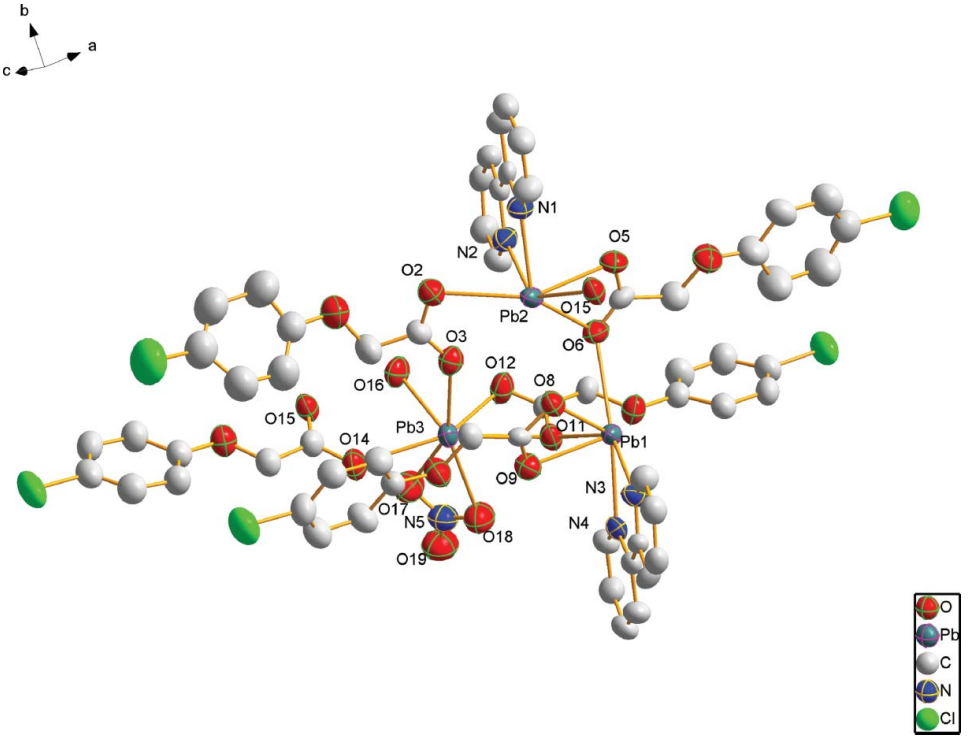

Figure 1. The coordination environment of **1**. Thermal ellipsoids are shown at 30% probability, all H atoms are omitted for clarity.

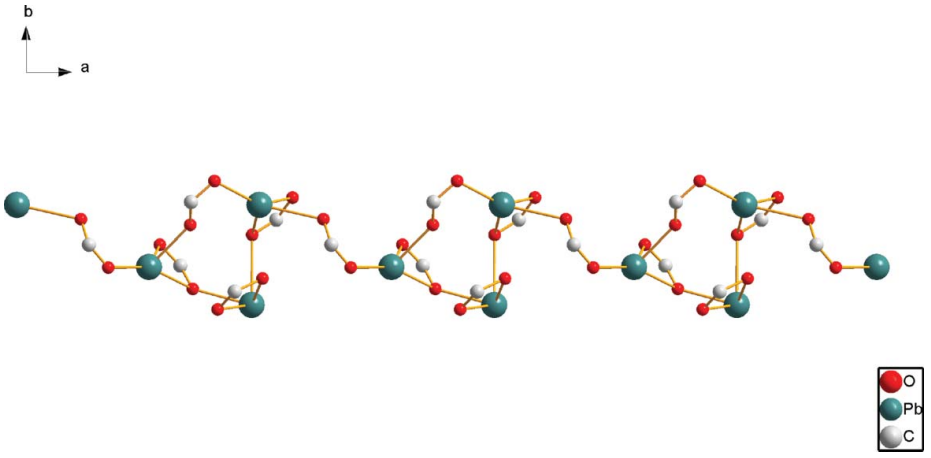

Figure 2. A view of 1D infinite chain construct with C–O–Pb. Unnecessary atoms are omitted for clarity.

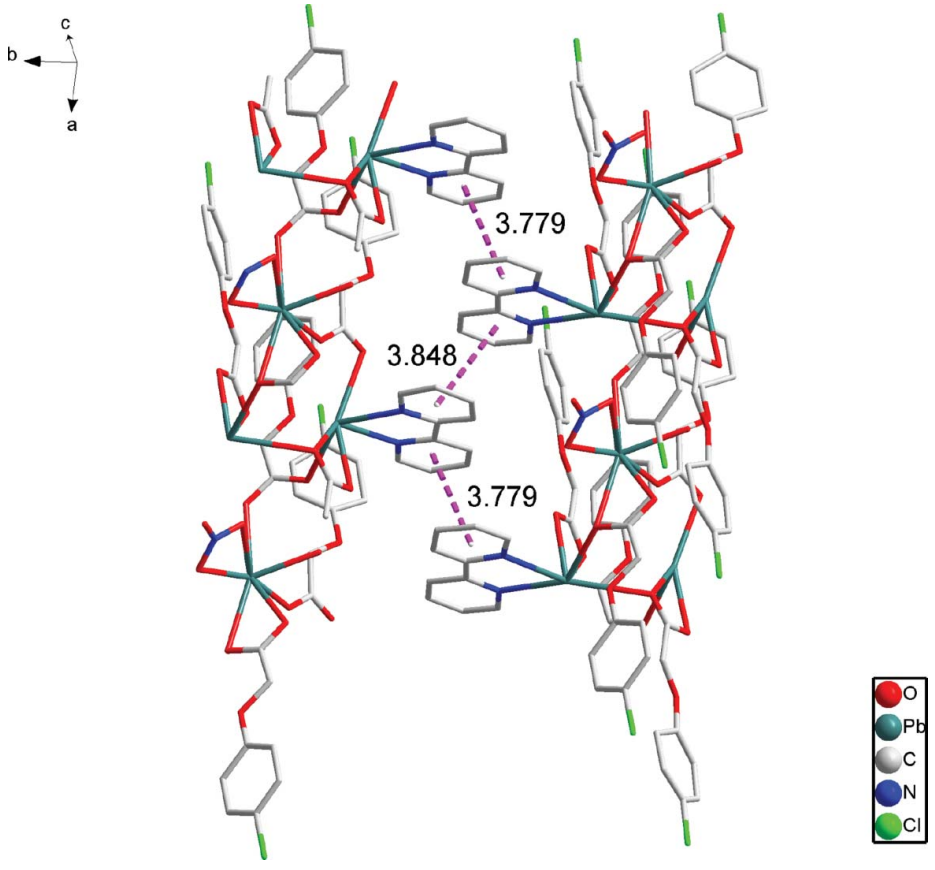

Figure 3. The 2D layered network of complex **1** via π–π stacking interactions. Unnecessary atoms are omitted for clarity.

Table 1. Crystallographic data for complex **1**, **2**, **3**, **4**, and **5**

Compounds	**1**	**2**	**3**	**4**	**5**
Empirical formula	$C_{60}H_{48}Cl_5N_5O_{19}Pb_3$	$C_{56}H_{40}Cl_4Cd_2N_4O_{12}$	$C_{56}H_{40}Cl_4Mn_2N_4O_{12}$	$C_{68}H_{52}Cl_6N_4O_{18}Mn_3$	$C_{16}H_{14}Cl_2O_7Pb$
Formula weight	1941.85	1327.52	1212.60	1590.66	596.36
Crystal system	Monoclinic	Triclinic	Triclinic	Triclinic	Monoclinic
Space group	*Cc*	*P*-1	*P*-1	*P*-1	*P*2(1)/*n*
a(Å)	9.765 (11)	8.457 (3)	8.458 (4)	10.621 (3)	6.502 (4)
b(Å)	24.09 (3)	15.739 (5)	15.606 (8)	12.753 (4)	7.422 (5)
c(Å)	27.27 (3)	20.968 (7)	20.856 (10)	13.110 (4)	37.87 (2)
α(°)	90	72.404 (4)	72.346 (8)	76.847 (5)	90
β(°)	97.041 (18)	83.487 (4)	83.528 (8)	88.142 (5)	91.915 (8)
γ(°)	90	82.708 (5)	82.784 (8)	76.518 (5)	90
V(Å^3)	6366 (13)	2630.6 (15)	2594 (2)	1681.1 (9)	1827 (2)
Z	4	2	2	1	4
D_c (Mg/m^3)	2.026	1.676	1.552	1.571	2.169
μ (mm^{-1})	8.202	1.080	0.762	0.869	9.565
F (000)	3704	1328	1236	809	1128
Crystal size (mm)	0.38 × 0.38 × 0.32	0.40 × 0.36 × 0.33	0.38 × 0.34 × 0.31	0.36 × 0.35 × 0.31	0.38 × 0.35 × 0.33
θ range	1.50–28.41	1.02–28.59	1.03–28.39	1.60–28.51	1.08 to 28.42
Reflections collected	20389	17335	16548	11239	11157
Independent reflections	10696 [*R*(int) = 0.0571]	11823 [*R*(int) = 0.0315]	11584 [*R*(int) = 0.1742]	7594 [*R*(int) = 0.0425]	4280 [*R*(int) = 0.0601]
Completeness to θ = 25.00	0.998	0.985	0.985	0.988	0.994
Absorption correction	Multi-scan	Multi-scan	Multi-scan	Multi-scan	Multi-scan
Max. and min. transmission	0.1789 and 0.1466	0.7169 and 0.6718	0.7980 and 0.7605	0.7745 and 0.7450	0.1444 and 0.1219
Data/restraints/parameters	10696/1348/829	11823/0/758	11584/0/758	7594/0/448	4280/32/235
Goodness-of-fit on F	1.034	1.031	0.842	0.934	1.174
R indices [$I > 2\sigma(I)$]	$R1 = 0.0517$, $wR2 = 0.1210$	$R1 = 0.0462$, $wR2 = 0.1078$	$R1 = 0.0583$, $wR2 = 0.1340$	$R1 = 0.0637$, $wR2 = 0.1737$	$R1 = 0.1115$, $wR2 = 0.3228$
R indices (all data)	$R1 = 0.0806$, $wR2 = 0.1329$	$R1 = 0.0928$, $wR2 = 0.1370$	$R1 = 0.2731$, $wR2 = 0.1790$	$R1 = 0.1355$, $wR2 = 0.2419$	$R1 = 0.1336$, $wR2 = 0.3416$
Largest diff. features (eÅ^{-3})	1.870 and –1.699	0.979 and –0.691	1.020 and –1.300	0.407 and –0.477	5.708 and –4.105

Table 2. The selected bond lengths (Å) and angles (°) for complex **1**, **2**, **3**, **4**, and **5**

Complex **1**			
Pb (1)–O(11)	2.474(11)	Pb(3)–O(18)	2.834(14)
Pb(1)–O(9)	2.492(12)	Pb(3)–O(17)	2.752(13)
Pb(1)–N(4)	2.567(13)	Pb(3)–O(11)	2.749(11)
Pb(1)–N(3)	2.591(13)	Pb(3)–O(14)	2.654(13)
Pb(1)–O(8)	2.673(11)	Pb(3)–O(3)	2.519(11)
Pb(1)-O(6)	2.884(11)	O(11)–Pb(1)–O(8)	101.5(3)
Pb(2)–N(1)	2.497(14)	O(9)–Pb(1)–O(8)	50.3(3)
Pb(2)–O(5)	2.499(13)	N(4)–Pb(1)–O(8)	120.0(4)
Pb(2)–N(2)	2.506(13)	O(5)–Pb(2)–O(2)	149.2(4)
Pb(2)–O(2)	2.666(12)	O(5)–Pb(2)–O(15)[a]	71.6(4)
Pb(2)–O(15)[a]	2.674(11)	N(2)–Pb(2)–O(6)	82.6(4)
Pb(2)–O(6)	2.702(12)	O(17)–Pb(3)–O(18)	44.5(4)
Pb(3)–O(12)	2.414(12)	O(16)–Pb(3)–O(14)	78.0(4)
Pb(3)-O(16)	2.463(11)	O(3)–Pb(3)–O(11)	92.4(4)
Complex **2**			
Cd(1)–O(3)	2.237(3)	Cd(2)–O(2)	2.315(3)
Cd(1)–O(10)	2.252(3)	Cd(2)–N(2)	2.400(4)
Cd(1)–O(5)	2.319(4)	Cd(2)–N(1)	2.404(4)
Cd(1)–O(8)	2.326(4)	O(3)–Cd(1)–O(10)	161.66(11)
Cd(1)–N(4)	2.385(4)	O(10)–Cd(1)–O(8)	84.41(14)
Cd(1)–N(3)	2.385(4)	N(4)–Cd(1)–N(3)	69.13(16)
Cd(2)–O(9)	2.242(4)	O(9)–Cd(2)–O(6)	163.85(12)
Cd(2)–O(6)	2.248(4)	O(11)–Cd(2)–O(2)	128.60(12)
Cd(2)–O(11)	2.296(4)	O(11)–Cd(2)–N(2)	149.48(13)
Complex **3**			
Mn(1)–O(3)	2.124(3)	Mn(2)–O(12)	2.195(3)
Mn(1)–O(11)	2.151(4)	Mn(2)–O(2)	2.217(4)
Mn(1)–O(9)	2.210(5)	Mn(2)–N(3)	2.341(4)
Mn(1)–O(5)	2.216(4)	Mn(2)–N(4)	2.345(5)
Mn(1)–N(2)	2.309(4)	O(3)–Mn(1)–O(11)	161.43(15)
Mn(1)–N(1)	2.316(5)	N(2)–Mn(1)–N(1)	70.71(17)
Mn(2)–O(6)	2.119(4)	O(12)–Mn(2)–O(2)	126.29(15)
Mn(2)–O(8)	2.137(4)	N(3)–Mn(2)–N(4)	70.14(14)
Complex **4**			
Mn(1)–O(8)	2.069(4)	Mn(2)–O(3)[a]	2.161(3)
Mn(1)–O(2)	2.103(4)	Mn(2)–O(9)[a]	2.196(4)
Mn(1)–O(5)	2.122(4)	Mn(2)–O(9)	2.196(4)
Mn(1)–N(2)	2.254(4)	O(2)–Mn(1)–O(5)	97.42(16)
Mn(1)–N(1)	2.266(4)	O(8)–Mn(1)–O(2)	106.59(16)
Mn(2)–O(6)	2.137(4)	O(6)–Mn(2)–O(3)	90.88(16)
Mn(2)–O(6)[a]	2.137(4)	O(3)–Mn(2)–O(9)	93.11(14)
Mn(2)–O(3)	2.161(3)	O(6)–Mn(2)–O(9)	88.06(15)
Complex **5**			
Pb(1)–O(5)	2.505(15)	Pb(1)–O(6)[b]	2.696(17)
Pb(1)–O(3)	2.51(2)	Pb(1)–O(2)[c]	2.711(16)
Pb(1)–O(7)	2.61(2)	O(5)–Pb(1)–O(6)	50.7(5)
Pb(1)–O(5)[a]	2.644(14)	O(5)–Pb(1)–O(6)[b]	118.3(5)
Pb(1)–O(6)	2.664(16)	O(6)–Pb(1)–O(2)[c]	147.6(5)

Symmetry transformations used to generate equivalent atoms:
[a]for Complex **1**: x + 1, y, z; [a]for Complex **4**: –x + 1, –y + 1,–z + 2;
[a]for Complex **5**: –x, –y + 1, –z; [b]for Complex **5**: –x, –y + 2, –z;
[c]for Complex **5**: x – 1, y, z.

Table 3. Hydrogen-bond geometry (Å) of complexes

D—H···*A*	*D*—H	H···*A*	*D*···*A*	*D*—H···*A*	Symmetry codes
Complex **1**					
O16–H16D···O5	0.850	2.02	2.859(16)	169.6	x – 1, y, z
O16–H16C···O12	0.850	1.98	2.825(17)	169.4	
Complex **5**					
O7–H7F···O5	0.850	2.37	3.20(3)	167.0	
O7–H7E···O3	0.850	2.04	2.87(3)	166.6	x – 1, y, z

diffraction-crystal module of the Mercury (Hg) program available free of charge via the Internet at http://www.iucr.org. Excitation and emission spectra were acquired on a Perkin–Elmer instruments LS55 spectrofluorometer.

Synthesis of the Complex $[Pb_3L_5(2,2'\text{-bipy})_2(NO_3)(H_2O)]_n$ **1**

A mixture of $Pb(NO_3)_2$ (165.5 mg, 0.3 mmol), HL (111.8 mg, 0.6 mmol), and 2,2′-bipy (46.2 mg, 0.3 mmol) were dissolved in the mixed solvent (1:1 H_2O/EtOH) (20 mL). Then, an aqueous solution of sodium hydroxide was added dropwise with stirring to adjust the pH value of the solution being 6. The mixture was kept heated at 130°C for 3 days. After

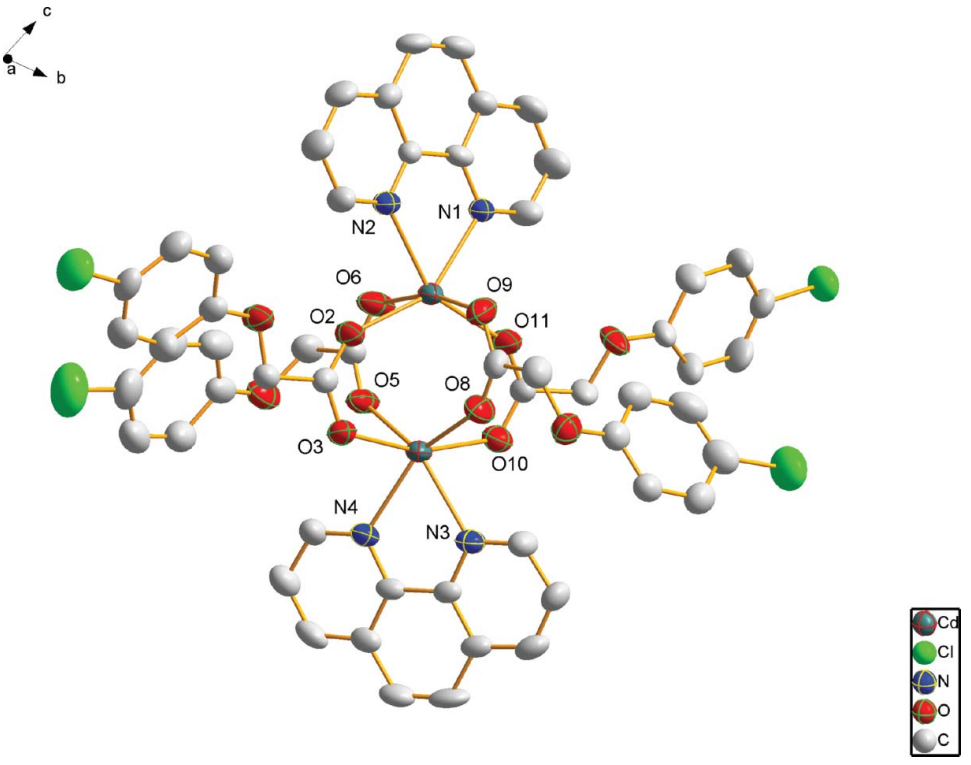

Figure 4. The coordination environment of **2**. Thermal ellipsoids are shown at 30% probability, all H atoms are omitted for clarity.

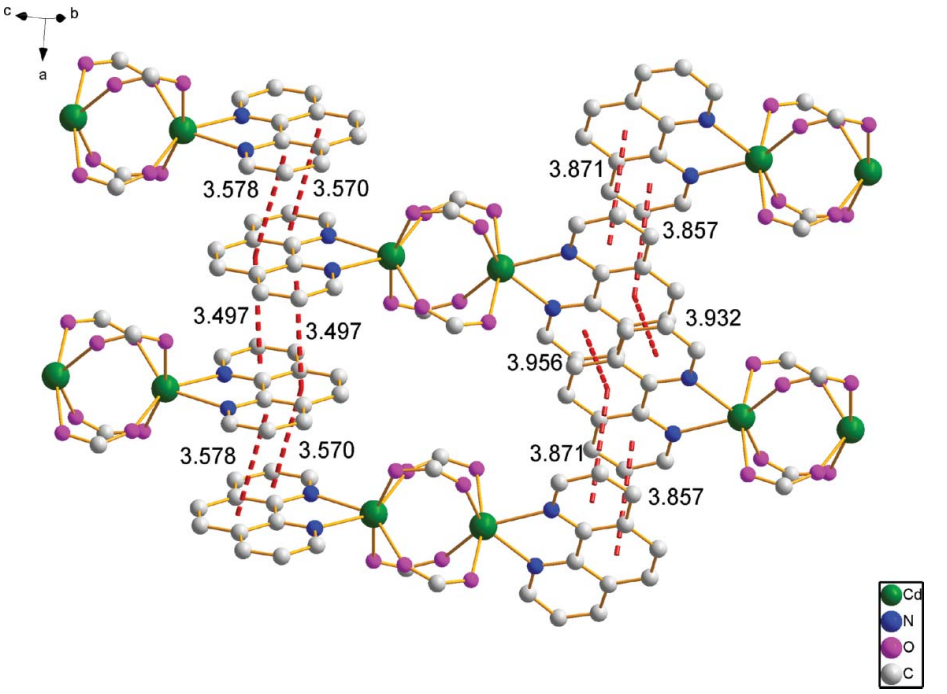

Figure 5. A view of 2D supramolecular structure and π–π stacking interactions of complex **2.** Unnecessary atoms are omitted for clarity.

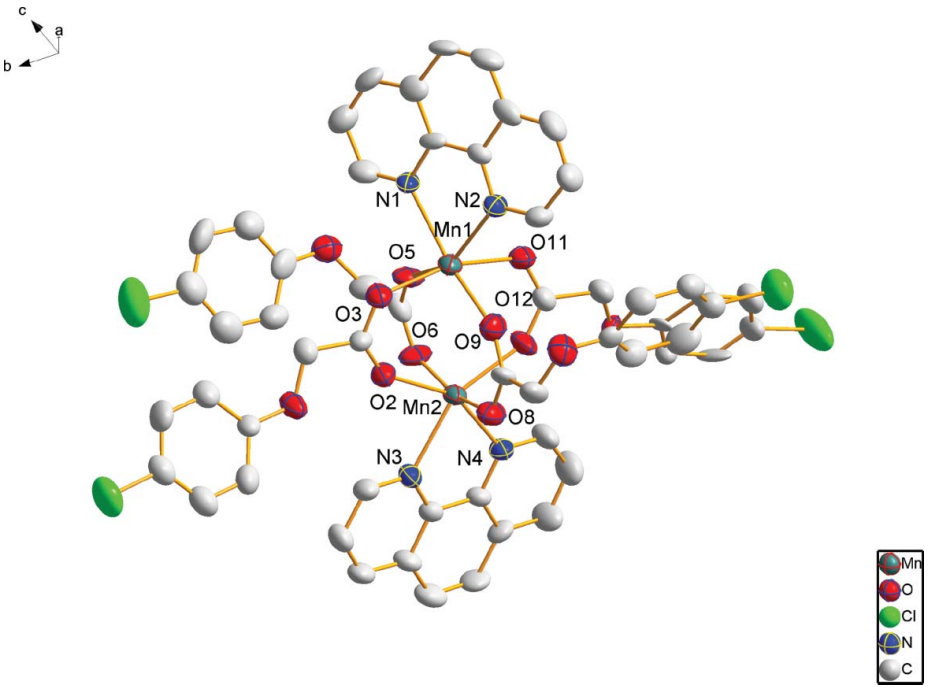

Figure 6. The coordination environment of **3**. Thermal ellipsoids are shown at 30% probability, all H atoms are omitted for clarity.

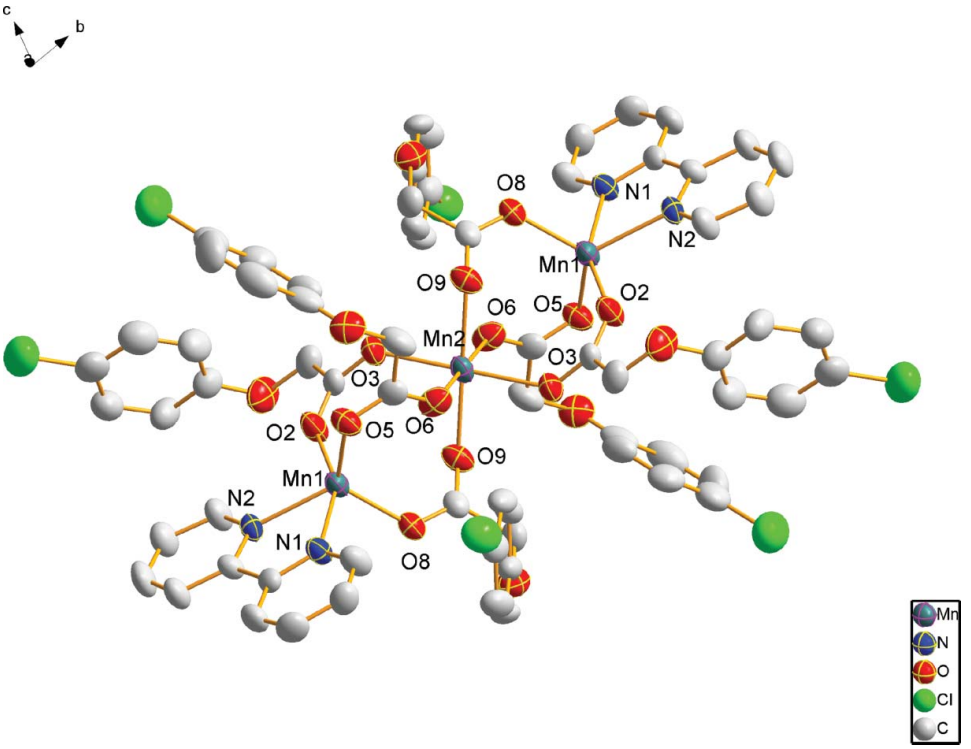

Figure 7. The coordination environment of **4**. Thermal ellipsoids are shown at 30% probability, all H atoms are omitted for clarity.

cooling to room temperature, the reaction solution was filtered to remove a small quantity of precipitation. Kept slow evaporation of the filtrate at room temperature and four days later X-ray quality colorless block-shaped single crystals were obtained. The crystals were isolated, washed with ethanol, and dried at room temperature (Yield: 55% based on Pb). Calcd. For $C_{60}H_{48}Cl_5N_5O_{19}Pb_3$: C 37.09, H 2.47, N 3.60%. Found: C 36.15,H 2.43, N 3.64%. IR (KBr, cm^{-1}): 3060 (w), 1618 (w), 1596 (s), 1491 (s), 1380 (s), 1242 (m), 821 (w), 724 (s).

Synthesis of the Complex $[Cd_2L_4(1,10\text{-Phenanthroline})_2]$ **2**

The synthesis of **2** was similar to that of **1** except that $CdCl_2{\cdot}2.5H_2O$ (68.4 mg, 0.3 mmol) was used instead of $Pb(NO_3)_2$ (165.5 mg, 0.3 mmol), and 2,2′-bipy (46.2 mg, 0.3 mmol) was replaced by 1,10-Phenanthroline (54 mg, 0.3 mmol). A week later, colorless block-shaped single crystals were obtained. The crystals were isolated, washed with ethanol, and dried at room temperature (Yield:70% based on Cd). Calcd.For $C_{56}H_{40}Cl_4Cd_2N_4O_{12}$: C 50.64, H 3.01, N 4.22%. Found: C 50.59,H 3.07, N 4.18%. IR (KBr, cm^{-1}): 3074 (w), 1662 (w), 1593 (s), 1492 (s), 1426 (s), 1244 (m), 822 (w), 726 (s).

Synthesis of the Complex $[Mn_2L_4(1,10\text{-Phenanthroline})_2]$ **3**

The synthesis of **3** was similar to that of **2** except that $MnCl_2{\cdot}4H_2O$ (58.2 mg, 0.3 mmol) was used instead of $CdCl_2{\cdot}2.5H_2O$ (68.4 mg, 0.3 mmol). Four days later, yellow block-shaped single crystals were obtained. The crystals were isolated, washed with ethanol, and dried at room temperature (Yield:65% based on Mn). Calcd.For $C_{56}H_{40}Cl_4Mn_2N_4O_{12}$: C 55.44, H 3.30, N 5.28%. Found: C 55.38,H 3.36, N 5.22%. 3082 (w), 1667 (s), 1593 (w), 1492 (s), 1429 (s), 1246 (m), 822 (w), 726 (s).

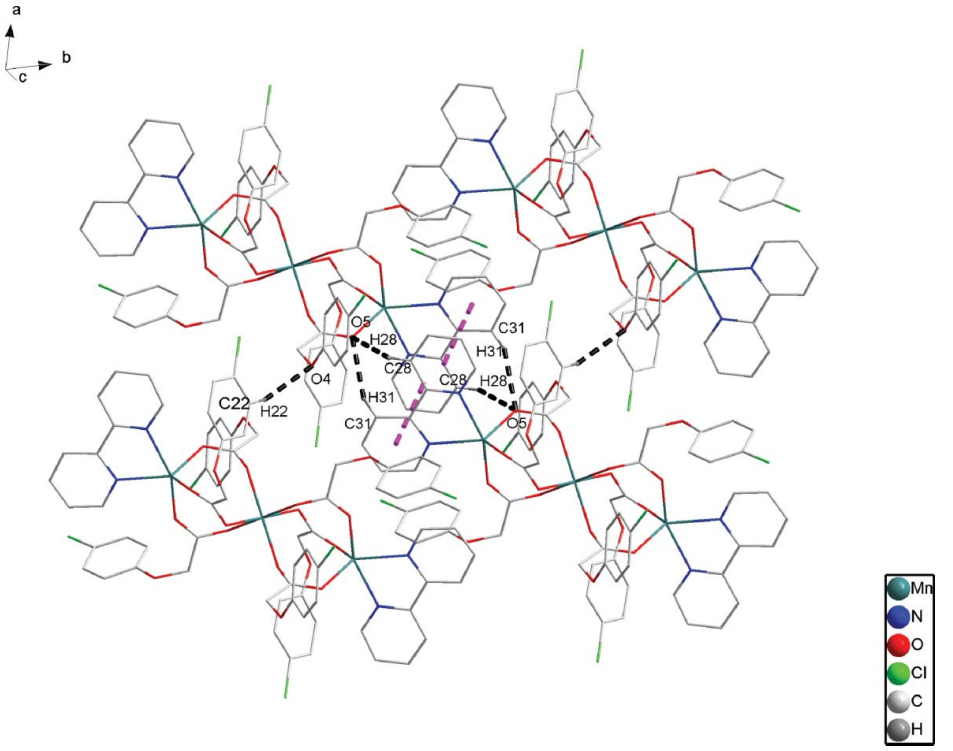

Figure 8. A perspective view of the 2D layered network via C–H···O and π–π stacking interactions.

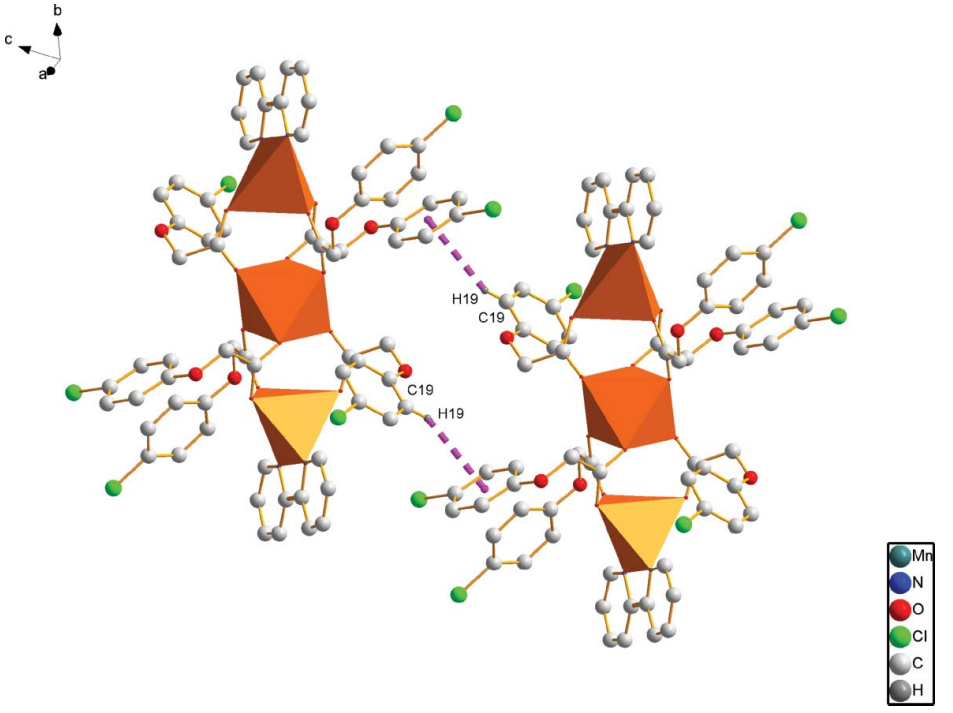

Figure 9. The weak C–H···π interaction in complex **4**.

Synthesis of the Complex $[Mn_3L_6(2,2'\text{-bipy})_2]$ **4**

A mixture of $MnCl_2{\cdot}4H_2O$ (58.2 mg, 0.3 mmol), HL (111.8 mg, 0.6 mmol), and 2,2′-bipy (46.2 mg, 0.3 mmol) were dissolved in the mixed solvent (1:1 H_2O/EtOH) (20 mL). Then, an aqueous solution of sodium hydroxide was added dropwise with stirring to adjust the pH value of the solution being 6. The mixture was kept heated at 130°C for 3 days. After cooling to room temperature, the reaction solution was filtered to remove a small quantity of precipitation. Kept slow evaporation of the filtrate at room temperature and four days later X-ray quality yellow block-shaped single crystals were obtained. The crystals were isolated, washed with ethanol, and dried at room temperature (Yield: 62% based on Mn). Calcd. For $C_{68}H_{52}Cl_6N_4O_{18}Mn_3$: C 51.32, H 3.27, N 4.02%. Found: C 51.28, H 3.24, N 3.99%. IR (KBr, cm^{-1}): 3116 (w), 1614 (s), 1598 (w), 1491 (s), 1411 (s), 1223 (m), 827 (m), 719 (w).

Synthesis of the Complex $[PbL_2(H_2O)]_n$ **5**

A mixture of $Pb(NO_3)_2$ (165.5 mg, 0.3 mmol) and HL (111.8 mg, 0.6 mmol) were dissolved in the mixed solvent (1:1 H_2O/EtOH) (20 mL). Using an aqueous solution of sodium hydroxide to adjust the pH value being 6. The mixture was kept heated at 130°C for 3 days. After cooling to room temperature, we get the colorless block-shaped single crystals. The X-ray quality crystals were isolated, washed with ethanol and dried at room temperature (Yield: 65% based on Pb). Calcd. For $C_{16}H_{14}Cl_2O_7Pb$: C 32.21, H 2.34%. Found: C 32.19, H 2.38%. IR (KBr, cm^{-1}): 3093 (w), 1619 (w), 1592 (w), 1492 (s), 1434 (m), 1239 (s), 821 (w), 720 (m).

X-Ray Data Collection and Structure Refinement

Crystallographic data of complexe was collected on a Bruker SMART CCD diffractometer with graphite monochromated Mo–Ka radiation ($\lambda = 0.71073$ Å) at $T = 296$ K.Absorption corrections were applied by using the multi-scan program [11]. The structure was solved by direct methods and successive Fourier difference syntheses (SHELXS-97), and anisotropic thermal parameters for all nonhydrogen atomswere refined by full-matrix least-squares procedure against F^2 (SHELXL-97) [12]. All nonhydrogen atoms were refined anisotropically. Hydrogen atoms were set in calculated positions and refined by a riding mode, with a common thermal parameter. H atoms for H_2O molecules were located in different synthesis and refined isotropically. Complex **2** and **3** are both have one disorder L ligand, in complex **3**, I did not set all hydrogens of the disorder L ligand, I just create some hydrogens and alter their occupancy to get the correct formula. The crystallographic data and experimental details for the structure analysis are summarized in Table 1, the selected bond lengths and angles are listed in Table 2, meanwhile, the hydrogen-bonds of the complexes are listed in Table 3.

Results and Discussion

Crystal Structure Descriptions

Single crystal X-ray analysis of **1** reveals that the asymmetric unit consists of three Pb(II) ions, two 2,2′-bipy, four L ligands, one NO_3^- anion, and one water. The Pb(II) ion in complex **1** has two kinds of coordination number, The Pb1 coordinate with two nitrogen atoms (N3, N4) from one 2,2′-bipy, with two oxygen atoms (O8, O9) from the carboxylate of L ligand and with two oxygen atoms (O6, O11) from the carboxylate of different two L ligands. Each Pb2 is coordinated by two nitrogen atoms (N1, N2) from one 2,2′-bipy, by

two oxygen atoms (O8, O9) from the carboxylate of L ligand and by two oxygen atoms (O2, O15) from the carboxylate of two different L ligands. The Pb3 coordinate with two oxygen atoms (O11, O12) from the a L ligand, with two oxygen atoms (O3, O14) from two different L ligands, with one oxygen atom (O16) from a coordinated water, and two oxygen atoms (O17, O18) from a NO_3^- anion. The different coordination number make each Pb1 and Pb2 adopt a distorted octahedral coordination, make Pb3 form a distorted decanedron coordination. We can see the environment of Pb in Fig. 1. The L ligand in complex **1** has three kinds of coordination modes: one is chelating, one displays a bridging bidentate, and the third adopts a bridging tridentate, which linked Pb ions together and extended in *a* axis direction to be a 1D chain (Fig. 2). The protrudent 2,2′-bipy molecules play an important role in structure construction as interlinkages by π–π stacking interactions with the phenyl rings from 2,2′-bipy molecules of adjacent chains into 2D supramolecular layer in *ab* plane. The centroid-to-centroid distances of π–π stacking interactions among the phenyl rings of 2,2′-bipy molecules and two phenyl rings of two neighboring 2,2′-bipy molecules are 3.779 and 3.848 Å (Fig. 3). In addition, the π–π stacking interactions also exist between two benzene rings of L ligands from adjacent layers (3.896 Å, 5.97°), which connected these 2D layers to be a 3D supermolecular structure. The hydrogen bonds in complex **1** also make the structure to be more stable.

As shown in Fig. 4 for compound **2**, all L ligands exhibit chelating bidentate arrangement. Compound **2** show us a 0D structure, there are two independent Cd(II) centers exist in the unit. Each Cd(II) adopts a slightly distorted octahedral coordination, are six coordinated by four oxygen atoms from the carboxylate of four different L ligands and two nitrogen atoms from one 2,2′-bipy. The nonbonding Cd1·Cd2 distance is 3.571 Å, four L ligands linked the two Cd(II) centers together through the chelating bidentate carboxylate. The two 1,10-phenanthroline coordinated with two Cd(II) at the opposite position, and the dihedral angle between them is 69.06°. There are π–π stacking interactions between the adjacent 1,10-phenanthroline of which the intercentroid distance being depicted in Fig. 5. These π–π stacking interactions construct complex **2** to be a two-dimensional supramolecular structure.

The X-ray structure shows that complex **3** has the same structure with compound **2**. The asymmetric unit of complex **3** consists of two Mn(II) ions, four L ligands and two 1,10-phenanthroline molecules. Each Mn(II) coordinate with four oxygen atoms from the carboxylate of four L ligands and two nitrogen atoms from a 2,2′-bipy (Fig. 6). The π–π stacking interactions also exist between the adjacent 1,10-phenanthroline, which paly an important part in the structure construction.

A perspective view of the molecular structure of the complex **4** along with the atom-numbering scheme is depicted in Fig. 7. The Mn(II) ion in complex **4** has two kinds of coordination number, each Mn1 coordinate with two nitrogen atoms (N1, N2) from one 2,2′-biphenyl and three oxygen atoms (O2, O5, O8) from three different bridging L ligands adopts a distorted hexahedron coordination, the Mn2 coordinate with six oxygen atoms from the carboxylate of six bridging bidentate L ligands show a slightly distorted octahedral coordination. The six L ligands linked three Mn ions together and make the structure become a dimer. The 0D dimer are linked by weak C31–H31···O5, C28–H28···O5, and C22–H22···O4 interactions and by π–π stacking to yield a layered network (Fig. 8). The 2D layers in complex **4** are packed alongside with eachother through weak C–H···π interactions (Fig. 9). Along with this shortest interaction (H19 to the centroid of ring C9–C14: 3.297 Å) propagating crystallographic *c* axis with the formation of a 3D supermolecule structure.

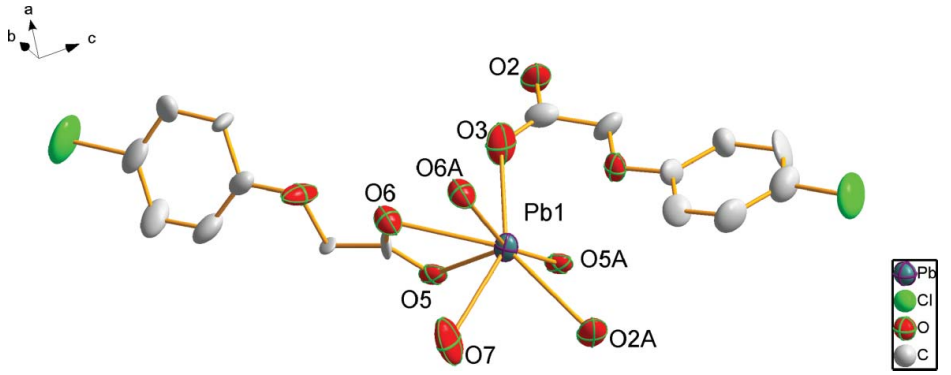

Figure 10. The coordination environment of **5**. Thermal ellipsoids are shown at 30% probability, all H atoms are omitted for clarity.

The X-ray structure shows that complex **5** adopts a 2D network polymer. The Pb(II) central atoms, which have decanedron coordination, are seven-coordinated by six oxygen atoms from five L ligands and one oxygen atom from a coordinated water (Fig. 10). The carboxylate group of L ligand exhibit bridging bidentate and chelating-bridging quadridentate modes. As shown in Fig. 11, complex **5** is stabilized through the C-O-Pb frame and weak O7–H7E···O3, O7–H7F···O5 hydrogen bonds.

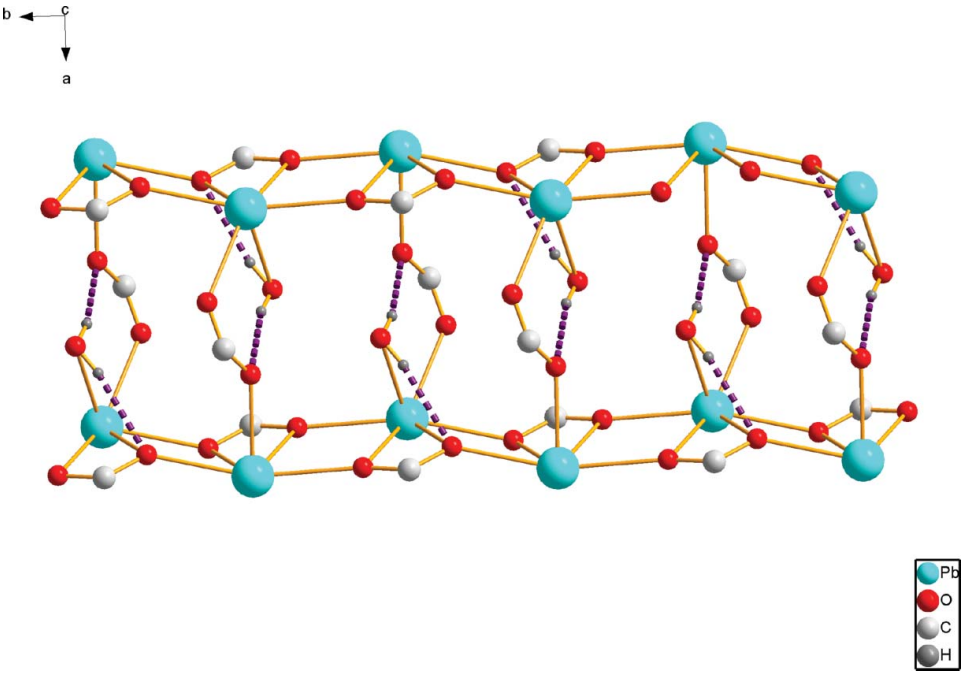

Figure 11. A perspective view of C–O–Pb frame and weak hydrogen bonds.

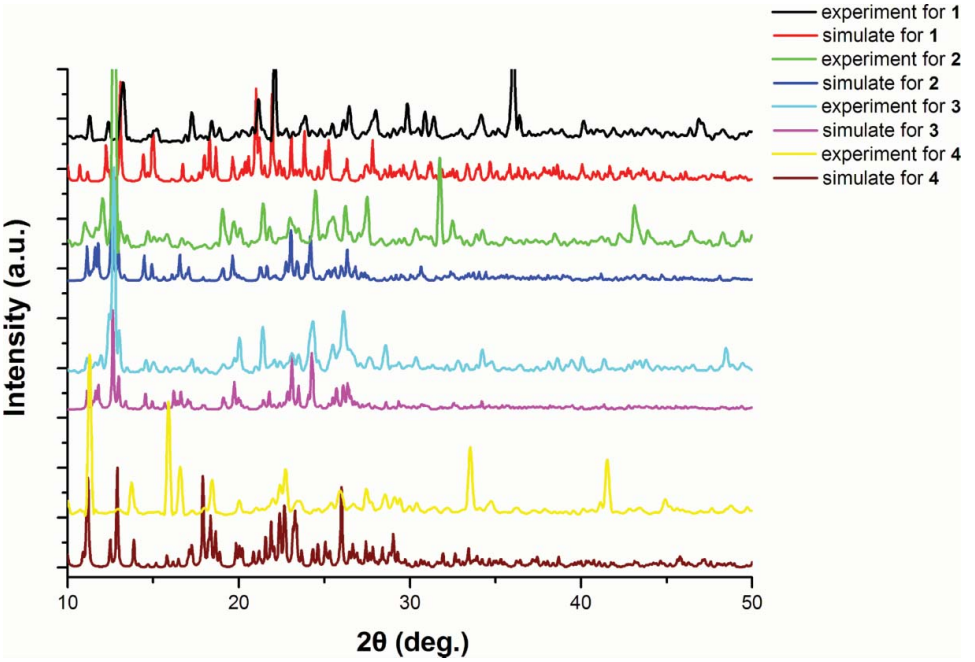

Figure 12. Simulated and experimental XRPD patterns for complex **1**, **2**, **3**, and **4**.

The structural consistency and phase purity of **1**, **2**, **3**, and **4** were confirmed by comparing the measured pattern calculated from single-crystal data with the experimental X-ray powder diffraction (XRPD) analysis at room temperature (Fig. 12).

IR Spectroscopy

The IR spectrum of complex **1**, **2**, **3**, **4**, and **5** are exhibit two peaks at 1618 cm^{-1} and 1380 cm^{-1}, 1662 cm^{-1} and 1426 cm^{-1}, 1667 cm^{-1} and 1429 cm^{-1}, 1614 cm^{-1} and 1411 cm^{-1}, 1619 cm^{-1} and 1434 cm^{-1}, respectively. which are assigned to the ν_{COO-} stretching vibration and indicate the coordination of the carboxylate group of L ligand to metal for the large red-shift compared with the IR spectrum of the free L ligand. The skeleton vibration bands of the phenyl ring appearing at 3060, 1596, and 1491 in **1**; 3074, 1593, and 1492 in **2**; 3082, 1593, and 1492 in **3**; 3116, 1598, and 1491 in **4**; and 3093, 1592, and 1492 in **5**. Furthermore, the band at around 822 cm^{-1} in all these complexes are attributable to the γ(=C–H) of 1, 4-substituted phenyl ring, and the peak at around 724 cm^{-1} can be attributed to the γ(–CH 2–) of the ligand.

Fluorescence Emission Properties

The photoluminescence behavior of the free ligand (HL) and its corresponding manganese (II), cadmium (II), plumbum (II) compounds were studied in the solution of methanol at room temperature. The excitation and emission spectra of **HL**, **1**, **2**, **3**, **4**, and **5** are depicted in Fig. 13. Upon photoexcitation at 288 nm, the free HL exhibits fluorescence emission at 310 nm. Upon excitation at 336 nm, the compound **1** show more intense photoluminescence with the main emission at 375 nm. Compound **2** exhibits emission around 370 nm upon excitation at 326 nm. Upon photoexcitation at 360 nm, compound **3** show a broad emission

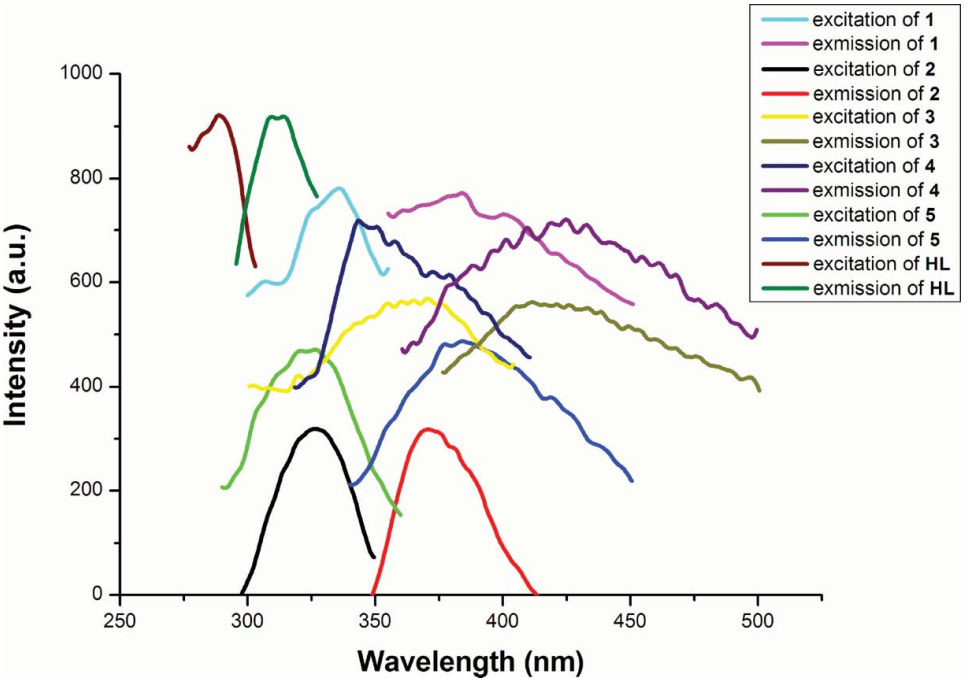

Figure 13. Photoluminescent spectrum of **HL** ligand and complex **1**, **2**, **3**, **4,** and **5** in the solution of methanol at room temperature.

peak at 410 nm. Compound **4** exhibits emission around 424 nm upon excitation at 343 nm. Upon photoexcitation at 322 nm, compound **5** exhibits fluorescence emission at 388 nm. The emission band for compound **1**, **2**, **3**, **4**, and **5** are different to that found for the free ligand in terms of position and band shape. Therefore, the luminescence behaviors in these complexes may be attributed to the intraligand (π–π^*) transition, and greater intensity may presumably be due to the increase in conformational rigidity of the ligand upon coordination. Meanwhile, compared with the emission spectrum of HL, a largely red shift in these five complexes have been observed, which is considered to mainly arise from the coordination effect of metal (II) with the ligand. Furthermore, the incorporation of metal (II) effectively increases the conformational rigidity of HL and reduces the loss of energy via vibration motions. Thus, the enhanced fluorescence intensities of the five compounds are detected.

Conclusion

This paper reports the synthesis and characterization of complexes $[Pb_3L_5(2,2'\text{-bipy})_2(NO_3)(H_2O)]_n$, $[Cd_2L_4(1,10\text{-Phenanthroline})_2]$, $[Mn_2L_4(1,10\text{-Phenanthroline})_2]$, $[Mn_3L_6(2,2'\text{-bipy})_2]$, and $[PbL_2(H_2O)]_n$ by IR method, elemental analysis, XRPD analysis, fluorescence spectroscopy method, and single-crystal X-ray diffraction techniques. The above results show that the configuration of ligand plays an important role in affecting the final structure of the coordination polymers. The successful preparation of the complexes manifest that the conformations and functions of π–π stacking interactions,

hydrogen bonds and van der Waals' forces are important factors in influencing the architecture of metal-L ligand complexes. In addition, Compound **1**, **2**, **3**, **4**, and **5** are all exhibits fluorescence in the solution of methanol at room temperature.

Supplementary Material

CCDC 904945, 904949, 904946, 904947, and 904948 contains the supplementary crystallographic data for this paper. These data can be obtained free of charge via www.ccdc.cam.ac.uk/conts/retrieving.html (or from the Cambridge Crystallographic Data Centre, 12, Union Road, Cambridge CB2 1EZ, UK; fax: C44 1223 336033; e-mail: deposit@ccdc.cam.ac.uk).

Acknowledgments

This work is supported by the Innovation Project of Guangxi University for Nationalities (gxun-chx2012089), the Scientific Research Program of Education Department of Guangxi Zhuang Autonomous Region (Project No. 201010LX081), and the Scientific Research Program of Guangxi University for Nationalities (Project No. 2010QD019).

References

[1] Yang, J. L., Seong, E. S., Kim, M. J., Ghimire, B. K., Kang, W. H., Yu, C. Y., & Li, C. H. (2010). *Plant Cell Tissue Organ Cult.*, *100*, 49.
[2] Castilla, A. M., Dauwe, T., Mora, I., Malone, J., & Guitart, R. (2010). *Bull. Environ. Contam. Toxicol.*, *66*, 101.
[3] Ratanasanobon, K., & Seaton, K. A. (2010). *Plant Cell Tissue Organ Cult.*, *100*, 59.
[4] Rakshit, S., Rashid, Z., Sekhar, J. C., Fatma, T., & Dass, S. (2010). *Plant Cell Tissue Organ Cult.*, *100*, 31.
[5] Aylward, L. L., Morgan, M. K., Arbuckle, T. E., Barr, D. B., Burns, C. J., Alexander, B. H., & Hays, S. M. (2010). *Environ. Health Perspect.*, *118*, 177.
[6] Ren, Y. X., Jiao, B. J., Zhang, M. L., Gao, X. M., & Wang, J. (2011). *Z. Anorg. Allg.Chem.*, *637*, 1612.
[7] Fomulu, S. L., Hendi, M. S., Davis, R. E., & Wheeler, K. A. (2002). *Cryst. Growth. Des.*, *2*, 637.
[8] Denderinou-Samara, C., Psomas, G., Raptopoulou, C. P., & Kessissoglou, D. P. (2001). *J. Inorg. Biochem.*, *83*, 7.
[9] Li, Z. P., Xing, Y. H., Cao, Y. Z., Zeng, X. Q., Ge, M. F., & Niu, S. Y. (2009). *Polyhedron.*, *28*, 865.
[10] Psomas, G., Dendrinou-Samara, C., Philippakopoulos, P., Tangoulis, V., Raptopoulou, C. P., Samaras, E., & Kessissoglou, D. P. (1998). *Inorg. Chim. Acta.*, *272*, 24.
[11] Blessing, R. H. (1995). *Acta Crystallogr A.*, *51*, 33.
[12] Sheldrick, G. M., SHELXTL97 Program for refining crystal structure refinement. University of Göttingen, Germany, 1997.